Journal of Power Sources 232 (2013) 270–278

Contents lists available at SciVerse ScienceDirect

Journal of Power Sources

journal homepage: www.elsevier.com/locate/jpowsour

# Dynamic modelling and parametric control for the polymer electrolyte membrane fuel cell system

Yuehong Zhao [a,*], Efstratios Pistikopoulos [b]

[a] State Key Laboratory of Multiphase Complex Systems, Institute of Process Engineering, Chinese Academy of Sciences, Beijing 100190, China
[b] Centre for Process Systems Engineering, Imperial College London, South Kensington Campus, London SW7 2AZ, UK

## HIGHLIGHTS

- A dynamic model for PEM fuel cell is developed and validated.
- The parametric controller is designed based on a solution to the model equations.
- The results show designed controller can optimize the PEM fuel cell operations.
- It ensures reliable performance in the presence of the current load fluctuations.

## ARTICLE INFO

*Article history:*
Received 4 September 2012
Received in revised form
18 December 2012
Accepted 20 December 2012
Available online 16 January 2013

*Keywords:*
Polymer electrolyte membrane fuel cell
Dynamic modelling
Parametric control
Multi-parametric programming

## ABSTRACT

This paper addresses the development of a parametric controller for the Polymer Electrolyte Membrane (PEM) fuel cell system, and the investigation of its performance. First, the dynamic modelling is carried out to obtain the transient performance of the PEM fuel cell system and to form the basis for the controller design. Then, a parametric controller is designed to optimize its operation, focussing on tracking the output voltage and stack temperature set points by suitably manipulating the oxygen and hydrogen excess ratios, and cooling water flow rate. It is realized by formulating a Model Predictive Control (MPC) problem, which is solved via parametric programming technique to obtain the explicit control action function. The closed-loop simulation results show that the designed parametric controller can track the set points well, and ensures reliable performance in the presence of the current load fluctuations. Compared to proportional–integral–derivative controller (PID), it has the advantages of satisfying the imposed constraints, the potential of simple hydrogen control operation and lower hydrogen consumption.



## 1. Introduction

PEM fuel cell is a device which can directly transfer chemical energy into electrical power with only heat and water as by-products if hydrogen is used as fuel source. It also shows the advantage to meet the demands for fast response under transient loads or cold start conditions, higher power density and lower operating temperature, which make it as a good candidate for clean electricity production for stationary and mobile applications.

To make it competitive to conventional power sources, many works have been devoted to studying PEM fuel cell system. In the field of modelling, there are many models have been proposed [1–3]. These models typically base on electrochemical reaction and physical characteristics of the inlet and outlet flows, providing useful knowledge about operation, dynamic response, and water and heat management [4–9]. In recent years, attempts have been made to study the control-oriented system-level modelling aiming to a better use of the fuel cell capacities and to the increase of the efficiency of the system. It was found that the input reactants flow and temperature show prominent impact on the performance of the PEM fuel cell system [10–15]. There are a number of control strategies, especially for air stream control, have been proposed, ranging from feedback control (PID), linear quadratic Gaussian (LQG), Neural Networks, and MPC [16–19]. Considering in most application cases the power demands fluctuate and then the fuel cell can't work at the optimal steady state designed by its manufacturer, which may make it in risk of starvation during high current demand and fast load changes. It is desired to suitably adjust the manipulated variables rapidly so that acceptable response time for the power demand and safe operation is ensured. For such

* Corresponding author. Tel.: +86 10 82612330; fax: +86 10 62554241.
*E-mail address:* yhzhao@home.ipe.ac.cn (Y. Zhao).

0378-7753/$ – see front matter © 2013 Elsevier B.V. All rights reserved.
http://dx.doi.org/10.1016/j.jpowsour.2012.12.116

control objective, MPC might be a good candidate for its ability to address multivariable problems with input and output constraints. However, MPC is limited to slowly varying processes due to the extensive on-line computational effort for solving the optimization problem. Hence, its application in PEM fuel cell system will be limited due to this drawback.

Parametric Model Predictive Control (pMPC) is a novel control technique, which overcomes the shortcoming of MPC's extensive on-line computation requirement while keeping same performance. Its novelty bases on the fact that it employs novel parametric programming technique to move off-line the on-line optimization problem involved in MPC. With this approach, the optimal control actions are obtained as explicit function of the state measurements. Moreover, its on-line implementation is simplified to a kind of simple state feedback controller and its on-line computational requirement is just to evaluate the functions. Hence, it suits to be used in the systems with fast dynamics or fast sampling time [20]. In this work, pMPC is proposed to manipulate the air, hydrogen and cooling water with aim of tracking the set points of output voltage and stack temperature to ensure reliable, smooth and efficient operations.

This paper is organized as follows: Section 2 and Section 3 describe the development and validation of the dynamic model. Section 4 shows parametric controller development and its performance investigation. Finally, the major conclusions are drawn in Section 5.

## 2. Fuel cell system model

A detailed dynamic model can help better understand the dynamic behaviour of PEM fuel cell system, and it is the central part of the controller design and evaluation. In this section, a system-level model is set-up for it is more suitable for system optimization and control [21]. In current work, major effort is put on PEM fuel cell's dynamic behaviour associated with the reactant flow, cooling water flow, and water phase change. Detailed model equations are described following sections. The following assumptions are considered for setting up the model equations:

(1) The Nafion-117 membrane is used,
(2) The fuel is pure hydrogen; compressed air is supplied as oxidant via an air compressor; and they will be ideally conditioned by a humidifier to certain humidity,
(3) No liquid water enters the gas channels,
(4) The gas is equally distributed in two gas supply channels, and the properties of flow exiting are same as those of the gas inside the channels,
(5) The fuel cell is well designed, and all cells in a stack perform similarly,
(6) Water condensation or evaporation rate is not considered. Instead, the equilibrium between water vapour and liquid water is assumed,
(7) Quasi-steady electrochemistry is assumed since the electrochemical reaction is rapid compared to mass and heat transfer,
(8) Gas is transported by diffusion, not convection through membrane,
(9) Auxiliary components are well controlled, ignoring their impacts on fuel cell behaviour, and
(10) They are integrated into anode and cathode volumes considering the relatively small volumes of manifolds of anode and cathode sides.

### 2.1. Fuel cell voltage model

For PEM fuel cell, many parameters, i.e. current load, reactant partial pressures, operating temperature, and membrane humidity, could affect its output voltage. Normally, It can be described as the difference between the open circuit and over-voltages as shown in Eq. (1), which has been extensively used in system-level fuel cell modelling [8,17,22–24].

$$V_{fc} = V_0 - V_{\text{act}} - V_{\text{ohm}} - V_{\text{conc}} \tag{1}$$

where $V_{\text{act}}$, $V_{\text{ohm}}$, and $V_{\text{conc}}$ are activation, ohmic and concentration over-voltages caused by the various physical and chemical factors; $V_0$ is the open circuit voltage and it can be expressed as

$$V_0 = 1.229 - 0.85 \times 10^{-3} \times \left(T_{fc} - 298.15\right) + 4.3085 \times 10^{-5} \times T_{fc} \times \left[\ln\left(P_{H_2}\right) + \frac{1}{2}\ln\left(P_{O_2}\right)\right] \tag{2}$$

where $T_{fc}$ is the fuel cell temperature, $p_{H_2}$ and $p_{O_2}$ are the partial pressures of $H_2$ and $O_2$ respectively.

In order to simplify the calculation, the activation over-voltage is described using an empirical model instead of Tafel expression [25].

$$V_{\text{act}} = \xi_1 + \xi_2 \cdot T_{fc} + \xi_3 \cdot T_{fc} \cdot \ln\left(c_{O_2}\right) + \xi_4 \cdot T_{fc} \cdot \ln\left(I\right) \tag{3}$$

where $\xi_i$ is the constant parametric coefficient; $I$ is current, $c_{O_2}$ is concentration of oxygen at the catalyst interface of cathode which can be got by ideal gas law.

The ohmic over-voltage and concentration over-voltage are described by following equations [8],

$$V_{\text{ohm}} = \frac{i \cdot t_{\text{mem}}}{\sigma_{\text{mem}}} \tag{4}$$

$$V_{\text{conc}} = -\frac{RT}{\alpha n \text{F}} \times \ln\left(1 - \frac{i}{i_{\max}}\right) \tag{5}$$

where $i$ and $i_{\max}$ are the actual and maximum current density; $t_{\text{mem}}$ is membrane thickness; $\sigma_{\text{mem}}$ is membrane proton conductivity and it is a function of the fuel cell working temperature $T_{fc}$ as listed below,

$$\sigma_{\text{mem}} = \sigma \cdot \exp\left[1268\left(\frac{1}{303} - \frac{1}{T_{fc}}\right)\right] \tag{6}$$

$$\sigma = 0.005139\lambda_{\text{mem}} - 0.00326 \tag{7}$$

where $\lambda_{\text{mem}}$ is the membrane water content, which is discussed in Section 2.4.

### 2.2. Mass balance in cathode

In cathode side, the humidified air is supplied through gas channel and gas diffusive layer (GDL) to catalyst layer where oxygen combines with protons and electrons to form water, at the same time the electricity and heat are generated. By employing mass conservation law, the dynamic of air supply can be expressed by the mass continuity of oxygen, nitrogen, and water (*l*, liquid and *v*, vapour) under condition of the given inlet flow rate [11,22].

$$\frac{dm_{O_2,ca}}{dt} = W_{O_2,\text{in},ca} - W_{O_2,\text{out},ca} - W_{O_2,\text{react}} \tag{8}$$

$$\frac{dm_{N_2,ca}}{dt} = W_{N_2,\text{in},ca} - W_{N_2,\text{out},ca} \tag{9}$$

$$\frac{dm_{v,ca}}{dt} = W_{v,\text{in},ca} - W_{v,\text{out},ca} + W_{v,\text{gen},ca} + W_{v,\text{mem}} + W_{\text{evap},ca} \quad (10)$$

$$\frac{dm_{l,ca}}{dt} = -W_{l,\text{out},ca} - W_{\text{evap},ca} \quad (11)$$

where $m$ is the mass of different gas species inside gas channel; $W$ is the corresponding mass flow rate, which are described as below.

In cathode side, the happened electrochemical reaction causes species mass changes, i.e. oxygen consumption and water generation. They are given by

$$W_{\text{O}_2,\text{react}} = M_{\text{O}_2} \times \frac{I}{4\text{F}} \quad (12)$$

$$W_{v,\text{gen},ca} = M_v \times \frac{I}{2\text{F}} \quad (13)$$

where F is Faraday Constant and $M$ is the molar mass of gas species.

In order to describe the equilibrium between water vapour and liquid water, $W_{\text{evap},ca}$ is defined. It is assumed positive in the case of the water vapour partial pressure is smaller than its corresponding saturation pressure, which causes water to evaporate. When the steam condenses, it is negative. It is described by Eq. (14) [22].

$$W_{\text{evap},ca} = \min\left(A_{fc}\left(P_{\text{sat}}\left(T_{fc}\right) - P_{v,ca}\right)\sqrt{\frac{M_v}{2\pi R T_{fc}}}, 0\right) \quad (14)$$

where $P_{v,ca}$ is the partial pressure of water vapour; $P_{\text{sat}}$ is the water saturated pressure at $T_{fc}$.

At the outlet, a linearized nozzle model is used to describe the cathode exit flow. Then, the mass flow rate of each species in cathode outlet can be got by Eqs. (15)–(19).

$$W_{\text{out},ca} = K_{\text{out},ca}\left(P_{ca} - P_{\text{out},ca}\right) \quad (15)$$

$$W_{\text{O}_2,\text{out},ca} = \frac{m_{\text{O}_2,ca}}{m_{ca}} \cdot W_{\text{out},ca} \quad (16)$$

$$W_{\text{N}_2,\text{out},ca} = \frac{m_{\text{N}_2,ca}}{m_{ca}} \cdot W_{\text{out},ca} \quad (17)$$

$$W_{v,\text{out},ca} = \frac{m_{v,ca}}{m_{ca}} \cdot W_{\text{out},ca} \quad (18)$$

$$W_{l,\text{out},ca} = -W_{\text{evap},ca} \quad (19)$$

In Eqs. (14)–(19), $K_{\text{out},\ ca}$ is valve coefficient; $A_{fc}$ is fuel cell effective area; $m_{ca}$ is the total mass of gas flow (oxygen, nitrogen and steam) inside cathode gas channel. $W_{v,\text{mem}}$ is the water flow rate across the membrane, which is described Section 2.4.

### 2.3. Mass balance in anode

In anode side, the humidified hydrogen is supplied through gas channel and gas diffusive layer (GDL) to catalyst layer where hydrogen dissociates into protons and electrons. The produced protons drag some water pass through membrane into cathode, while the electrons collect on the anode electrode surface and flow in external circuit to the cathode. By employing similar method used for cathode side modelling, mass continuity equations in anode side can be obtained as following.

$$\frac{dm_{\text{H}_2,an}}{dt} = W_{\text{H}_2,\text{in},an} - W_{\text{H}_2,\text{out},an} - W_{\text{H}_2,\text{react}} \quad (20)$$

$$\frac{dm_{v,an}}{dt} = W_{v,\text{in},an} - W_{v,\text{out},an} - W_{v,\text{mem}} + W_{\text{evap},an} \quad (21)$$

$$\frac{dm_{l,an}}{dt} = -W_{l,\text{out},an} - W_{\text{evap},an} \quad (22)$$

where

$$W_{\text{evap},an} = \min\left(A_{fc}\left(P_{\text{sat}}\left(T_{fc}\right) - P_{v,an}\right)\sqrt{\frac{M_v}{2\pi R T_{fc}}}, 0\right) \quad (23)$$

$$W_{\text{H}_2,\text{react}} = M_{\text{H}_2} \times \frac{I}{2\text{F}} \quad (24)$$

By assuming the condensed liquid water in the anode is dragged out by the exit gas flow instantly, outlet flow rate of each species can be described by Eqs. (25)–(28).

$$W_{\text{out},an} = K_{\text{out},an} v_{\text{out},an}\left(P_{an} - P_{\text{out},an}\right) \quad (25)$$

$$W_{\text{H}_2,\text{out},an} = \frac{m_{\text{H}_2,an}}{m_{an}} \cdot W_{\text{out},an} \quad (26)$$

$$W_{v,\text{out},an} = \frac{m_{v,an}}{m_{an}} \cdot W_{\text{out},an} \quad (27)$$

$$W_{l,\text{out},an} = -W_{\text{evap},an} \quad (28)$$

where $v_{\text{out},\ an}$ is stage of outlet valve. If anode gas channel is dead end, then $v_{\text{out},an} = 0$, else $v_{\text{out},an} = 1$. $m_{an}$ is the total mass of gas flow (hydrogen and steam) inside anode.

### 2.4. Mass transfer between anode and cathode

Membrane Electrolyte Assembly (MEA) is the bridge between the anode and the cathode, providing the physical environment for electrochemical reaction and species mass transport. Modelling of water transport across membrane is the major objective of MEA model under condition of assumed quasi-steady electrochemical reaction.

The water vapour ($v$) transport across the membrane is mainly achieved by two effects, the electro-osmotic driving forces caused by the electrochemical potential difference between the cathode and anode, and the back-diffusion caused by the water vapour concentration gradient across the membrane. Combining these two transport mechanisms, the water flow across the membrane from anode to cathode can be written as [22],

$$W_{v,\text{mem}} = M_v A_{fc}\left(\frac{n_d I}{F} - D_w \frac{c_{v,ca} - c_{v,an}}{t_{\text{mem}}}\right) \quad (29)$$

where $n_d$ is the number of water molecules carried by each proton, and it can be given by Eq. (30); $D_w$ is the membrane diffusion coefficient, which varies with membrane water content $\lambda_{\text{mem}}$ as described in Eq. (31); $c_{v,i}$ ($i \in [an,ca]$) represents the water vapour ($v$) concentration at the membrane surfaces, which are functions of water ($v$) content on the surface ($\lambda_i$) and can be described as $c_{v,i} = \rho_{\text{mem,dry}}\lambda_i / M_{\text{mem,dry}}$, where $\rho_{\text{mem,dry}}$,$M_{\text{mem,dry}}$are the dry membrane density and membrane dry equivalent weight; $\lambda_i$ is the average water content at the anode and cathode, which is the function of the membrane water ($v$) activity $a_i$($i \in [an,ca]$).

Following are the model equations used to calculate these parameters for the Nafion-117 membrane. [26]

$$n_d = 0.0029\lambda_{\text{mem}}^2 + 0.05\lambda_{\text{mem}} - 3.4\times10^{-19} \tag{30}$$

$$D_w = D_\lambda \exp\left(2146\left(\frac{1}{303}-\frac{1}{T_{fc}}\right)\right) \tag{31}$$

$$\lambda_i = \begin{array}{ll} 0.043 + 17.81a_i - 39.85a_i^2 + 36a_i^3 & 0 < a_i \le 1 \\ 14 + 1.4(a_i - 1) & 1 < a_i \le 3 \\ 16.8 & 3 < a_i \end{array} \tag{32}$$

$$D_\lambda = \begin{array}{ll} 10^{-6} & \lambda_{\text{mem}} < 2 \\ 10^{-6}(1 + 2(\lambda_{\text{mem}} - 2)) & 2 \le \lambda_{\text{mem}} < 3 \\ 10^{-6}(3 - 1.67(\lambda_{\text{mem}} - 3)) & 3 \le \lambda_{\text{mem}} < 4.5 \\ 1.25\times10^{-6} & \lambda_{\text{mem}} \ge 4.5 \end{array} \tag{33}$$

### 2.5. Energy balance model

With the aim of obtaining the temperature of PEM fuel cell stack, the energy balance model is set-up according to the conservation of energy. In current work, $q_{\text{in},an}$ and $q_{\text{in},ca}$ are defined to describe the heat carried in by the hydrogen and air streams; $q_{\text{out},an}$ and $q_{\text{out},ca}$ are defined to describe the heat carried out by outlet streams. Moreover, the heat and electrical power generated by the electrochemical reaction ($q_{\text{react}}$, $q_{\text{elec}}$), heat released/absorbed due to water phase change inside the fuel cell ($q_{l-v}$), and the heat loss ($q_{\text{loss}}$) which is mainly transferred to surroundings by the natural convection and to coolant [9,27] are also considered. All these energy items decide the net heat ($q_{\text{net}}$) accumulated to heat up fuel cell stack. Hence, overall energy balance is expressed as,

$$q_{\text{in},an} + q_{\text{in},ca} + q_{\text{react}} + q_{\text{elec}} + q_{l-v} + q_{\text{net}} + q_{\text{loss}} = q_{\text{out},ca} + q_{\text{out},an} \tag{34}$$

Following are the detailed discussion about the energy flows involving the overall energy balance calculation.

For a PEM fuel cell stack, heat loss can be estimated by the average loss from the surface to the environment via $q_{\text{loss}} = h_{\text{cell}}A_{\text{cell}}(T_{fc}-T_{\text{room}})$ under condition of no cooling system. If cooling system is installed, the heat taken out by which should also be considered as part of $q_{\text{loss}}$. In current work, the water cooling is adopted. The heat transfer to cooling water is described by.

$$q_{\text{sens},cw} = N_{cw}C_{p,cw}(T_{cw,\text{out}} - T_{cw,\text{in}}) \tag{35}$$

where $N_w$ is cooling water flow rate; $C_{p,cw}$ is the cooling water specific heat capacity;

$T_{cw,\text{out}}$ is the outlet temperature of cooling water which can be obtained using the Eq. (36) by assuming the cooling water temperature is the half between input and output [9].

$$T_{cw,\text{out}} = 2\left[T_{fc} - \frac{q_{\text{sens},cw}}{(hA)_w}\right] - T_{cw,\text{in}} \tag{36}$$

The heat carried in by input streams is described as,

$$q_{\text{in},an} = \sum_i W_{i,\text{in},an}C_{p,i,\text{in},an}(T_{\text{in},an} - T_0) \tag{37}$$

$$q_{\text{in},ca} = \sum_i W_{i,\text{in},ca}C_{p,i,\text{in},ca}(T_{\text{in},ca} - T_0) \tag{38}$$

Similarly, the heat carried out by outlet streams is described as,

$$q_{\text{out},an} = \sum_i W_{i,\text{out},an}C_{p,i,\text{out},an}(T_{\text{out},an} - T_0) \tag{39}$$

$$q_{\text{out},ca} = \sum_i W_{i,\text{out},ca}C_{p,i,\text{out},ca}(T_{\text{out},ca} - T_0) \tag{40}$$

where $i$ represents the specie appears in input and output streams.

For simplicity, the electrical power generated by the fuel cell is expressed as $q_{\text{elec}} = V_{fc}\cdot I$. The available power released by the electrochemical reaction is assumed to be equal to the Gibbs free energy of the reaction.

$$q_{\text{react}} = \Delta G_{\text{react}} \tag{41}$$

where $\Delta G_{\text{react}}$ is the Gibbs free energy, which is given by,

$$\Delta G_{\text{react}} = \Delta G^0 - RT\ln\left[P_{H_2}P_{O_2}^{0.5}/P_{\text{vap},ca}\right] \tag{42}$$

The latent heat caused by the water phase change includes two parts, $q_{l-v,an}$ and $q_{l-v,ca}$. In anode side, $q_{l-v,an}$ can be obtained by $q_{l-v,an} = W_{\text{evap},an}\cdot H_{\text{cond}}$ by assuming no liquid water entering the gas channels and no reaction products in gas state, where $H_{\text{cond}}$ is the water vapour condense heat. Similarly, $q_{l-v,ca}$ can be obtained.

When the fuel cell operates at steady stage, the accumulated net heat $q_{\text{net}}$ is 0. However, during the transitions, the temperature of the fuel cell will change due to the accumulated net heat. It can be described as

$$m_{fc}C_{fc}\frac{dT_{fc}}{dt} = q_{\text{net}} \tag{43}$$

where $m_{fc}C_{fc}$ is the fuel cell stack specific heat capacity. By solving this equation, the temperature of fuel cell and outlet cooling water can be obtained under different operating conditions.

## 3. Model validation

The developed model is implemented in Simulink environment based on the above discussions. Given a set of operating conditions (i.e., initial temperature, input flow rate, current load) and parameters of fuel cell system (i.e., channel volume, MEA physical properties), the model can predict dynamic information regarding the start-up, transient response to step current load and input reactant flow rate change of a PEM fuel cell stack. In current work, it is assumed a fuel cell stack with 35 cells connected in a series to be modelled. The values of parameters used in simulation are

**Table 1**
Parameters used in the model validation.

| Parameters | Value | Parameters | Value |
|---|---|---|---|
| $T_{\text{room}}$ | 296.15 K | $T_{\text{mem}}$ | 0.001275 cm |
| $T_{\text{init}}$ | 296.15 K | $i_{\max}$ | 1.5 A cm$^{-2}$ |
| $n$ | 35 | $M_{m,\text{dry}}$ | 1.1 kg mol$^{-1}$ |
| $(\text{hA})_{\text{room}}$ | 17 W K$^{-1}$ | $\rho_{m,\text{dry}}$ | 0.002 kg cm$^{-3}$ |
| $M_{\text{fc}}C_{\text{fc}}$ | 35000 J K$^{-1}$ | $\text{RH}_{\text{an}}$ | 1 |
| $T_{\text{in}}$ | 296.15 K | $\text{RH}_{\text{ca}}$ | 0.5 |
| $A_{\text{eff}}$ | 280 cm$^2$ | $K_{\text{an,valve}}$ | 1 |
| [a]$K_{\text{out,an}}$ | 0.0001 kg bar$^{-1}$.s | Pin | 2.4 bar |
| [a]$K_{\text{out,ca}}$ | 0.005 kg bar$^{-1}$.s | [a]Excess $H_2$ ratio | 1.3 |
| $V_{\text{an}}$ | 0.005 m$^3$ | [a]Excess $O_2$ ratio | 2 |
| $V_{\text{ca}}$ | 0.01 m$^3$ | [a]$(\text{hA})_{cw}$ | 150 W K$^{-1}$ |
| $\xi_1$ | −0.944 | $\xi_2$ | 0.00354 |
| $\xi_3$ | 0.0000768 | $\xi_4$ | −0.000196 |

Note: For all cases, the anode and cathode inlet pressures are assumed to be kept at 2.4 bar; the Naffion-117 is used as the membrane.
[a] Parameters are specified based on assumption.

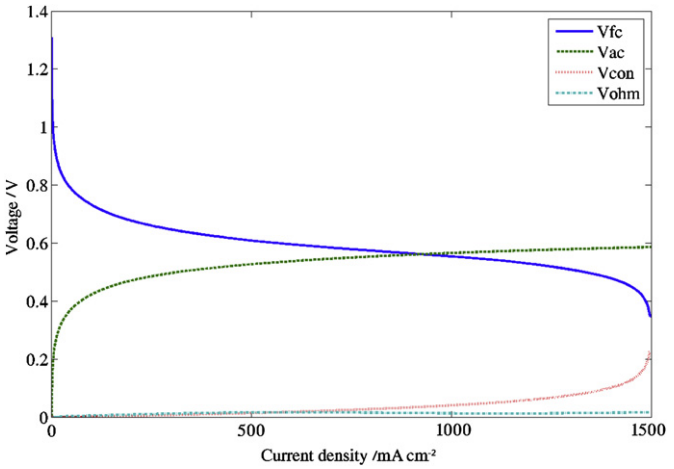


**Fig. 1.** Polarization curve at 353.15 K.

summarized in Table 1, which are taken from literature [27–29]. Some unavailable parameters are assumed according to literature [11,27–29]. For simplicity, it is assumed that fuel cell stack is ideally controlled at 353.15 K, which is the commonly used operating temperature. The input reactant flow rates of air and fuel are reflected by oxygen excess ratio $\lambda_{air}$ and hydrogen excess ratio$\lambda_{H_2}$, assuming they can be ideally controlled. In order to avoid starvation, oxygen excess ratio and hydrogen excess ratio are kept at 2 and 1.3, respectively.

In this work, a series of simulations are performed to validate the model and to study its dynamic responses. Fig. 1 shows the polarization curve of the fuel cell stack operated at the condition listed in Table 1. The qualitative trends of plots are similar to the typical $V$–$I$ curves, showing the decreasing output voltage due to rising over-voltage corresponding to the increasing current density; the rising activation and ohmic over-voltages due to increasing needs to move protons and electrons and to form and break chemical bonds, and membrane resistance to electrons transfer related to higher current load. It could also be seen that concentration over-voltage increases significantly with steep decline of output voltage when the current density approaches limiting current density (1500 mA $cm^{-2}$), which qualitatively agrees with the published reports [29]. Furthermore, the dynamic response analysis of fuel cell to current load is carried out using this model. As shown in Fig. 2, during a positive current step changes, more oxygen and hydrogen will be consumed which causes a drop in the stack output voltage as a result but with a quick recovery, while an increase in stack output voltage corresponding to a negative current step. The results agree with the typical operation characteristics of PEM fuel cell.

**Table 2**
Parameter for parametric controller design.

| Controller characteristics | Process data |
|---|---|
| Input variables | Simulation duration: $t = 2000$ s |
| Hydrogen excess ratio $\lambda_{H_2}$ | Nominal values: |
| Oxygen excess ratio $\lambda_{O_2}$ | $[V_b\ T_b] = [19.5353.15]$ |
| Cooling water flow $F_{cw}$ | Constraints |
| Disturbance variable | $1.2 \le \lambda_{H_2} \le 1.5$ |
| Current load $I$ | $1.2 \le \lambda_{O_2} \le 1.5$ |
| Output variable | $0 \le F_{cw} \le 100$ |
| Output voltage $V_{st}$ | $V_{st} - V_b \le 2.5$ |
| Stack temperature $T_{st}$ | $T_{st} - T_b \le 5$ |
| Controlling objective: | |
| Adjusting the hydrogen and oxygen excess ratios and cooling water flow to ensure output voltage and stack temperature reach preset values | Current load $I = 280$A + disturbance |

## 4. Parametric model-based control of PEM fuel cell system

In this section, a parametric controller is designed to optimize the PEM fuel cell stack operation, which focuses on tracking the output voltage and temperature signals via suitable manipulation of the fuel, reactant and cooling water flow rates under the condition of different current loads as measured disturbance.

The above developed model forms the basis for the controller design. However, an accurate but simple description of the complex PEM fuel cell system is still needed. Hence, model identification and reduction methodologies are employed, which are implemented via system identification toolbox of Matlab using data from simulations using step change of input variables, i.e. oxygen excess ratio $\lambda_{O_2}$, hydrogen excess ratio $\lambda_{H_2}$, current load $I_{st}(A)$, and cooling water flow rate $F_{cw}$(g $s^{-1}$) around their nominal values (2.0, 1.3, 280, 30), while other operating parameters keep fixed as listed in Table 1. The obtained model is,

$$\begin{cases} x_{t+1} = Ax_t + Bu_t + Cd_t \\ y_t = Dx_t \end{cases}$$

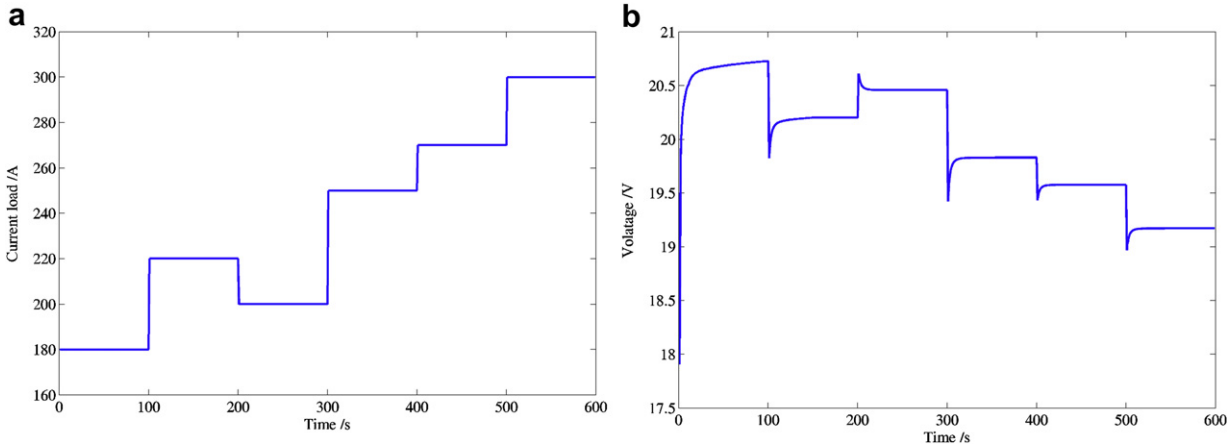


**Fig. 2.** The dynamic response of fuel cell to step current load (a) step current load; (b) Output voltage.

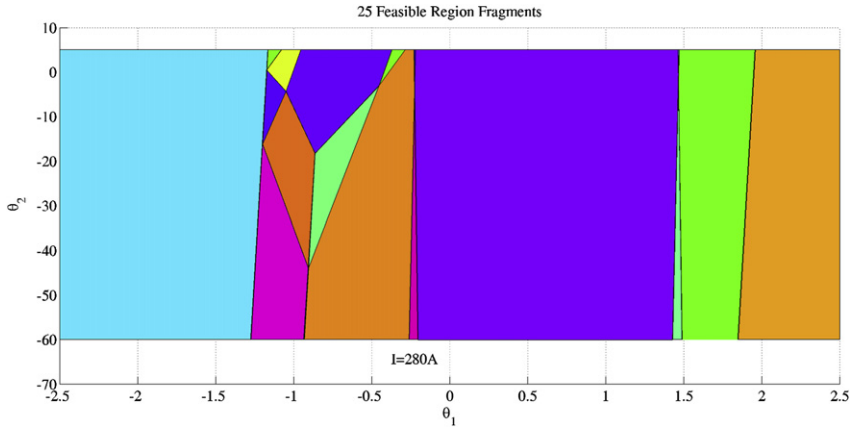


**Fig. 3.** Critical regions of the closed-loop parametric controller.

In this model, are state variables defined as the deviations of output voltage $V_{st}$ and stack temperature $T_{st}$ to their corresponding nominal values ($V_b = 19.5V$, $T_b = 353.15$ K), which help suppress the steady sate offset; $u_t = [\lambda_{H_2} \lambda_{O_2} F_{cw}]^T$ are the manipulated variables; $d_t$ and $I_{st}$ represents input disturbance and varying power demands respectively. The sample time of 1 s is considered in current work. The discrete state space matrices *A, B, C, D* are calculated as,

$$A = \begin{bmatrix} 0.67881 & 0.00054284 \\ -0.031704 & 0.99666 \end{bmatrix} \quad B = \begin{bmatrix} 0.36629 & 0.22968 & 0.0054877 \\ -1.8470 & 0.033292 & 0.00043003 \end{bmatrix}$$

$$C = \begin{bmatrix} -0.004148 \\ 0.00068905 \end{bmatrix} \quad D = \begin{bmatrix} 1 & 0 \\ 0 & 1 \end{bmatrix}$$

Then an MPC problem is formulated to optimize the PEM fuel cell operations, aiming to minimize the tracking errors of output $y_t$, to keep smooth moves of control effort $u_t$, and to satisfies the underlying operating constraints. The MPC cost function is given by

$$\min_{y,u} J = \sum_{k=1}^{N-1} \left(y_k - y^R\right)' QR \left(y_k - y^R\right) + \sum_{k=0}^{M-1} u_k' R u_k$$

where *QR* is the weighting factor on tracking error between the controller output $y_k$ and its desired value $y^R$ which is assumed fixed at **0**; *R* is the weighting factor on the controller input $u_k$; *N* and *M* are the prediction horizon and control horizon respectively. By observing the controller performance, *N, M, QR* and *R* are tuned. A prediction horizon *N* of 5 and control horizon *M* of 2 give a good controller performance. The corresponding optimal control weighting factors of *QR* and *R* are as follows,

$$QR = \begin{bmatrix} 1000000 & 0 \\ 0 & 1000 \end{bmatrix} \quad R = \begin{bmatrix} 100 & 0 & 0 \\ 0 & 100 & 0 \\ 0 & 0 & 0.1 \end{bmatrix}$$

The imposed constraints for the MPC problem involves lower and upper bounds for inputs and outputs of the controller, which include oxygen excess ratio ($1.5 \le \lambda_{O_2} \le 3.0$), hydrogen excess ratio ($1.2 \le \lambda_{H_2} \le 1.5$), cooling water flow rate ($0\ g\ s^{-1} \le F_{cw} \le 100\ g\ s^{-1}$), output voltage deviation to the nominal value ($\le$2.5 V), and stack temperature deviation to its nominal value ($\le$5 K). In order to

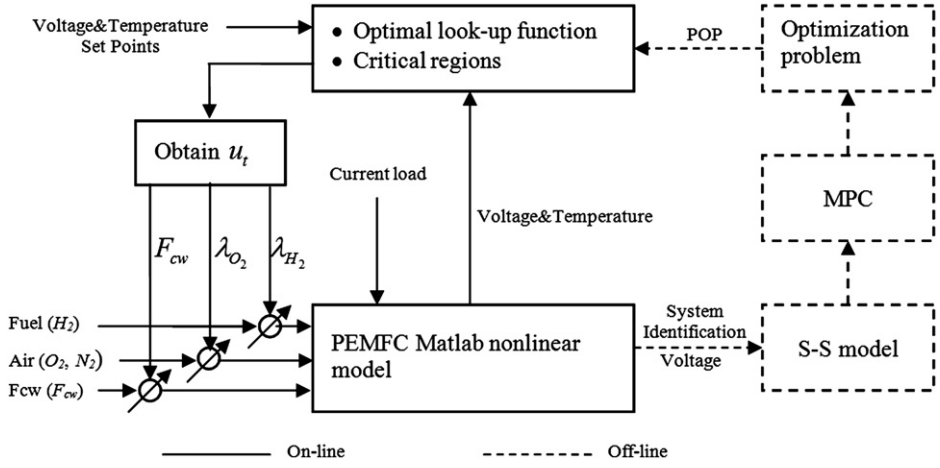


**Fig. 4.** Schematic diagram of parametric control system.

represent power demand fluctuations, the current load is assumed between 250 *A* and 310 *A*.

The above formulated MPC problem is then recast as a parametric optimization problem and solved off-line using parametric optimization technique. The parameters used for calculation are listed in Table 2. The resulting parametric control law for the case with current load of 280*A* results in partition of state space into 25 critical regions (CR) as shown in Fig. 3. Associated with each critical region is a control law that is an affine function of the state variables of $V_{st} - V_b$ and $T_{st} - T_b$. The implementation of the controller is just to identify the CR according to the states $x_t$ and then to compute the optimal oxygen excess ratio $\lambda_{O_2}$, hydrogen excess ratio $\lambda_{H_2}$ and cooling water flow rate $F_{cw}$, which is much easier and time-saving to compute than solving an on-line MPC optimization problem. Moreover, this controller can be embedded as a Matlab function in Simulink and integrated on-line with the developed dynamic fuel cell model to form a closed-loop system. A schematic diagram of parametric control system is shown in Fig. 4.

In order to investigate the performance of the designed parametric controller to optimize the PEM fuel cell operations, i.e. tracking set points and reject disturbance, a series of closed-loop simulations are carried out using the operating condition as listed in Table 1. Considering the much slower heat transfer compared to electrochemical reaction and big temperature gap between the start (293.15 K) to the desire point (353.15 K), it is impossible to make voltage and temperature simultaneously track the set points during start-up period. Therefore, it is assumed that no control action is adopted to adjust temperature before temperature reaches 352.15 K, and which period is defined as start-up stage.

The closed-loop simulation is first conducted at fixed current load at 280 *A* for 1000 s to make sure fuel cell is sufficiently heated to reach the temperature around set point. Then, a series of step changes of current loads, representing different power demands, are used to study the controller's ability rejecting disturbance. As the same time, the classic PID control strategy is also designed to further validate the parametric controller.

### 4.1. Performance of pMPC in start-up stage

As shown in Fig. 5, the stack temperature increases slowly, and it needs about 180 s to settle in (Fig. 5(b)) due to much slower heat transfer caused by the high thermal mass and large heat capacity of the stack. It can be found in Fig. 5(c) that the voltage reaches the set point within 200 s and tracks the set point well, with deviation less than 0.25%. Fig. 5(d,e) show the corresponding profiles of manipulated hydrogen and oxygen excess ratios. It can be found that the

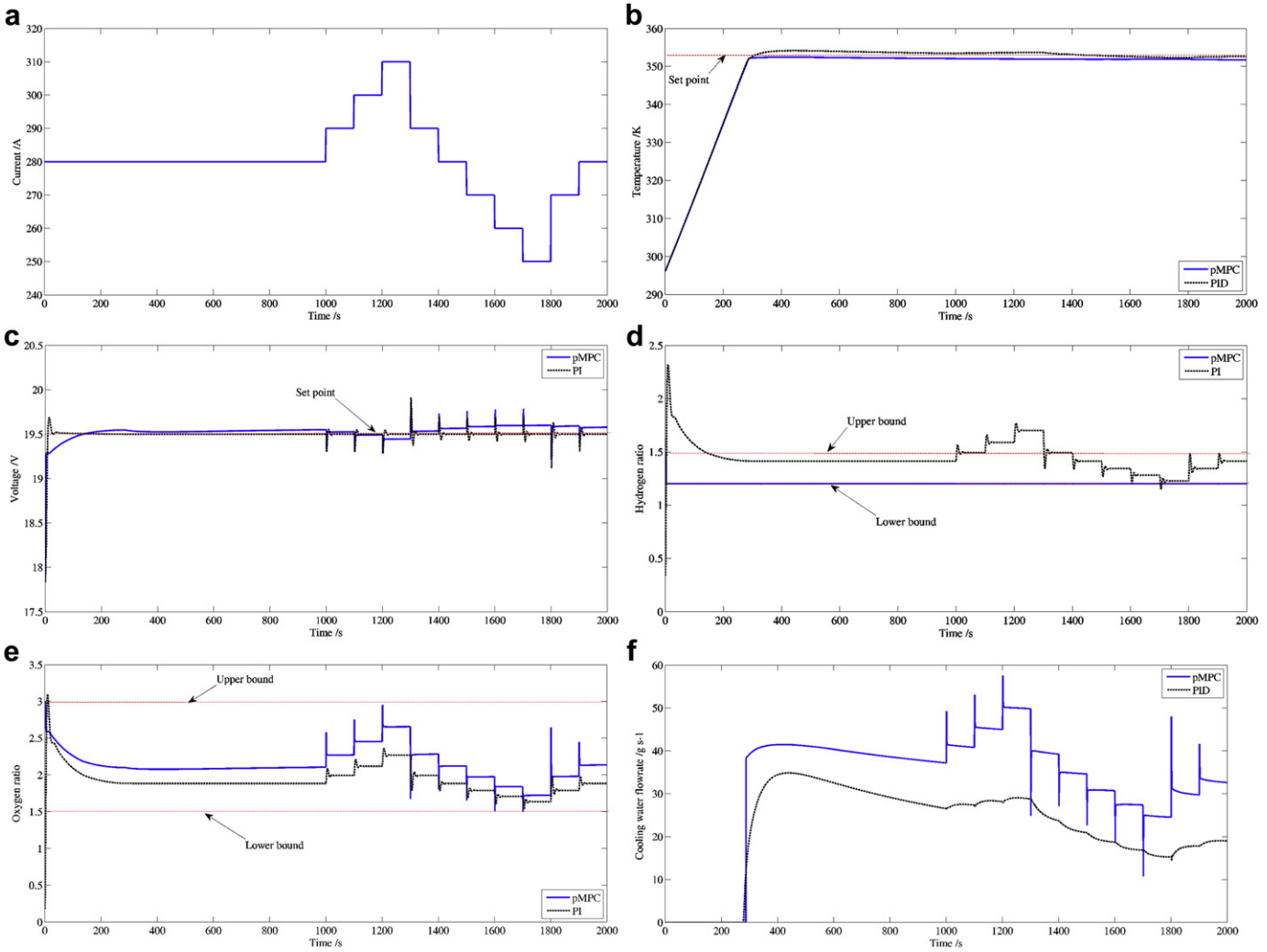


**Fig. 5.** Performance of parametric controller and it comparisons with PID (a) step current load; (b) output voltage profile; (c) stack temperature profile; (d), (e) hydrogen & oxygen excess ratio profiles; (f) cooling water flow rate profile.

hydrogen excess ratio is kept at 1.2 in most of operating time except start-up at 1.5 as initial input, while oxygen excess ratio is continually adjusted to keep fuel cell system working at set points. This result agrees with the common control strategy focussing on adjusting air flow to achieve demand output voltage for PEM fuel cell system [12]. Fig. 5(f) shows the profile of cooling water flow rate, cooling water is not used until stack temperature reaches set point, and then keeps changing to keep stack temperature around set point smoothly. As a result, the cooling of the stack is effective.

### 4.2. Performance of pMPC under disturbance

To study parametric controller's ability to reject the disturbance, a series of disturbances of current loads (Fig. 5 (a)) are used in the simulation. It can be observed (Fig. 5(b,c)) that the parametric controller achieves rapid disturbance rejection, taking about 5 s to restore to set point with less than 0.5% deviation, under conditions of current load disturbances between $-30$ *A* and $+30$ *A* while keep the stack temperature with little fluctuation. Fig. 5(d–f) show the profiles of manipulated hydrogen and oxygen excess ratios and cooling water flow rate. It can be found that the moves for all the manipulated variables are kept within the constraints.

### 4.3. Comparison of parametric controller and PID

To further validate the parametric controller, the classic PID control strategy is adopted to control the hydrogen and oxygen excess ratios, and cooling water flow rate respectively. For simplicity, it is assumed the cooling water is adjusted to control the stack temperature, while the hydrogen and oxygen excess ratios are adjusted to control output voltage. It should be noted that different control actions might be obtained due to such assumption. The PID controllers are tuned by observing the closed-loop simulation results. The resulting controllers are as follows,

For hydrogen excess ratio control,

$$K_{p,\mathrm{H_2}} = 0.2,\ K_{I,\mathrm{H_2}} = 0.3;$$

For oxygen excess ratio control,

$$K_{p,\mathrm{O_2}} = 0.1,\ K_{I,\mathrm{O_2}} = 0.4;$$

For cooling water control,

$$K_{p,cw} = -10,\ K_{I,cw} = 0.003,\ K_{D,cw} = 1.$$

As shown in Fig. 5, it can be found that parametric control and PID control strategies both can track the set points very well, but PID shows faster start-up and better disturbance rejection ability for output voltage under higher current load disturbance with the price of breaking the input constraints on hydrogen and oxygen excess ratios. While parametric controller keep all the inputs in the constraints, and shows faster response to the disturbance and better stack temperature tracking performance, which are helpful to keep reliable operations.

As shown in Fig. 5(d, e), different control strategies are adopted. PID control strategy adjusts the hydrogen and oxygen excess ratios simultaneously responding to the output voltage deviation to the set point, keeping higher hydrogen excess ratio, but lower oxygen excess ratio compared to parametric controller. Parametric control strategy only adjusts oxygen excess ratio while keeps hydrogen excess ratio at 1.2 in most of operation time, which means the simple control operation and less hydrogen consumption. For cooling water control, it can be found in Fig. 5(f) that PID control strategy needs less cooling water because of neglecting the imposed constraints and slower response.

## 5. Conclusions

In this paper, a parametric controller is proposed to optimally control the PEM fuel cell with the aim of tracking the output voltage and operating temperature set points. The advantages of this controller are that it reduces on-line computation effort by moving offline the on-line MPC optimization problem, and can provide optimal inputs as explicit function of states of fuel cell stack. The work includes two major parts, the control-oriented model development and parametric controller set-up.

First, a general control-oriented dynamic model for PEM fuel cell is developed to study its dynamic response under different operating conditions. The validation study shows that developed model can capture the general and dynamic behaviour of the PEM fuel cell system, and can be used as the basis for controller design. Then, an MPC problem is formed, which is recast as a parametric optimization problem and solved via parametric programming technique to obtain the optimal control law. The closed-loop simulations show that parametric controller tracks the set point well, and shows good performance under current load fluctuations. Compared to PID, it shows the advantages of satisfying the imposed constraints, and the potential of simple hydrogen control operation and lower hydrogen consumption.

## Acknowledgements

This work was partially sponsored by the Scientific Foundation for the Returned Overseas Chinese Scholars, State Education Ministry. The author would like to thank Professor Efstratios Pistikopoulos at Centre for Process Systems Engineering (CPSE), Imperial College, for his valuable comments and guidance throughout this work during author's 1-year visiting at CPSE. The author also would like to thank Dr. Konstantinos Kouramas at CPSE for his kind help in this work.

## References

[1] C.-Y. Wang, Chemical Review 104 (2004) 4727–4776.
[2] C. Bao, M. Ouyang, B. Yi, International Journal of Hydrogen Energy 31 (2006) 1879–1896.
[3] M. Matzopoulos, Fuel Cell Focus (2007) 44–47.
[4] D. Chen, H. Peng, Modeling and simulation of a PEM fuel cell humidification system, in: Proceeding of the 2004 American Control Conference (2004). Boston, Massachusetts.
[5] Y. Shan, S.-Y. Choe, Journal of Power Sources 158 (2006) 274–286.
[6] P. Badrinarayan, PEM Fuel Cell Water and Thermal Management: A Methodology to Understand Water and Thermal Management in an Automotive Fuel Cell System, University of California, 2001.
[7] S. Yu, D. Jung, Renewable Energy 33 (2008) 2540–2548.
[8] M. Grotsch, M. Mangold, Chemical Engineering Sciences 63 (2008) 434–447.
[9] X. Yu, B. Zhou, A. Sobiesiak, Journal of Power Sources 147 (2005) 184–195.
[10] S. Varigonda, M. Kamat, Computer and Chemical Engineering 30 (2006) 1735–1748.
[11] J.T. Pukrushpan, H. Peng, A.G. Stefanopoulou, Measurement, and Control 126 (2004) 14–25.
[12] A.P. Vega-Leal, F. Rogelio, F. Barragan, Journal of Power Sources 169 (2007) 194–197.
[13] S.-Y. Choe, J.-G. Lee, J.-W. Ahn, et al., Journal of Power Sources 164 (2007) 614–623.
[14] J.T. Pukrushpan, A.G. Stefanopoulou, H. Peng, Modeling and control for PEM fuel cell stack system, in: Proceedings of the American Control Conference (2002). Anchorage, AK.
[15] C. Bao, M. Ouyang, B. Yi, International Journal of Hydrogen Energy 31 (2006) 1897–1913.
[16] C. Bordons, A. Arce, A.J.d. Real, Constrained predictive control strategies for PEM fuel cells, in: Proceedings of the 2006 American control conference (2006). Minneapolis, Minnesota, USA.
[17] M.A. Danzer, J. Wilhelm, H. Aschemann, et al., Journal of Power Sources 176 (2008) 515–522.
[18] J. Golbert, D.R. Lewin, Journal of Power Sources 135 (2004) 135–151.
[19] J. Golbert, D.R. Lewin, Journal of Power Sources 173 (2007) 298–309.
[20] E.N. Pistikopoulos, M.C. Georgiadis, V. Dua (Eds.), Theory and Applications. Multi-parametric Model-based Control, vol. 2, Wiley-VCH, 2007.
[21] C. Bao, M. Ouyang, B. Yi, Journal of Power Sources 156 (2006) 232–243.
[22] A.J.d. Real, A. Arce, C. Bordons, Journal of Power Sources 173 (2007) 310–324.
[23] G. Maggio, V. Recupero, L. Pino, Journal of Power Sources 101 (2001) 275–286.

[24] J.C. Amphlett, R.M. Baumert, R.F. Mann, et al., Journal of Power Sources 49 (1994) 349–356.
[25] R. O'Hayre, S.-W. Cha, W. Colella, et al., Fuel Cell Fundamentals, Wiley, 2005.
[26] S.-K. Park, S.-Y. Choe, Journal of Power Sources 179 (2008) 660–672.
[27] P.R. Pathapati, X. Xue, J. Tang, Renewable Energy 30 (2005) 1–22.
[28] X. Xue, J. Tang, A. Smirnova, et al., Journal of Power Sources 133 (2004) 188–204.
[29] J. Larmine, A. Dicks, Fuel Cell Systems Explained, second ed., Wiley-VCH, 2003.

## Nomenclature

*A:* area ($cm^2$)
*a:* water activity
$C_p$: specific heat capacity ($J\ kg^{-1}K^{-1}$)
*F:* Faraday Constant (96485 coulombs)
*h:* heat transfer coefficient ($W\ m^{-2}K^{-1}$)
*i:* current density ($mA\ cm^{-2}$)
*I:* current (A)
*m:* mass (kg)
*M:* molar mass ($g\ mol^{-1}$)
*N:* molar flow rate ($mol\ s^{-1}$)
*n:* number of cells in stack
*P:* pressure (bar)
*q:* energy flow rate ($J\ s^{-1}$)
*R:* universal gas constant ($J\ mol^{-1}K^{-1}$)
*t:* thickness (cm) or time (s)
*T:* temperature (K)
*V:* voltage (V) or volume ($m^3$)
*W:* mass flow rate ($kg\ s^{-1}$)

*Subscripts*
*act:* activation
*an:* Anode
*ca:* cathode
*cell:* proton exchange membrane cell
*conc:* concentration
*cw:* cooling water
*elec:* electrical energy
*evap:* evaporation
*fc:* fuel cell
*gen:* generated
*i:* index
*in:* inlet
*l:* liquid
*mem:* membrane
*ohm:* ohmic
*out:* outlet
*sat:* saturation
*sens:* sensible heat
*st*:* stack
*v:* vapour

*Greek letters*
$\xi$: constant parametric coefficient
$\rho$: Density ($kg\ cm^{-3}$)
$\sigma$: membrane proton conductivity ($\Omega^{-1}cm^{-1}$)
$\lambda$: water content or ratio